



# Performance Improvement and Two-Phase Flow Study of a Piezoelectric Micropump with Tesla Nozzle-Diffuser Microvalves

S. Derakhshan<sup>†</sup>, B. Beigzadeh, M. Rashidi and H. Pourrahmani

*Iran University of Science and Technology 1, Tehran, 16846-13114, Iran*

<sup>†</sup>*Corresponding Author Email: [shderakhshan@iust.ac.ir](mailto:shderakhshan@iust.ac.ir)*

(Received April 19, 2017; accepted September 4, 2018)

## ABSTRACT

The Present article aims to design a piezoelectric micropump using a combinational form of microvalves with sufficient diodicity in low-pressure gradients. The goal is to enhance the capability of piezoelectric micropumps with Tesla-type valves in order to deliver insulin. Tesla-type valves are in the category of passive valves which have sufficient diodicity in case of high-pressure gradients. However, low mass flow rates are often required in drug delivery devices. In this paper, the performance of MT135 Tesla-type valve in low pressure-gradient flows has been investigated and a range of reunion angles, which have not been studied before has been examined by numerical solutions. Inspired by nozzle-diffuser valve types, some changes in the bypass path of the microvalve have been exerted to boost the diodicity of the valve in low-pressure conditions that resulted in 9.97% increase of diodicity. At last but not least, the velocity gradients in single-phase flow of water has been attained and performance of micropump toward other kinds of flows has been investigated by a volume of fluid (VOF) model including water as the primary phase and air as the secondary one. To complete the analysis, a VOF model consisting of an arbitrary kind of Casson fluid with the primary phase of water was reached and discussed.

**Keywords:** Micropump; Piezoelectric; Tesla-type valve; Nozzle-diffuser valve; Multiphase flow.

## NOMENCLATURE

$D_i$	diodicity	$U$	fluid velocity
$K_C$	square root of the Casson plastic viscosity	$\rho_f$	density
$K_{0C}$	square root of the yield stress	$\mu_f$	dynamic viscosity
$P$	pressure	$Q$	flow rate

## 1. INTRODUCTION

Nowadays, devices with small dimensions have eased the life and boost the precision of various scientific operations. Transporting fluids in micro orders of the volume have drawn researchers' attention toward investigating and designing microsystems, which micropumps have been one of the outstanding examples among the most important devices in micro-engineering. Drug delivery has been one of the basic goals of developing micropumps. Immunity is a vital feature of micropumps with drug delivery application which makes them perfectly feasible to disperse insulin or

other fluidic drugs into the human body. The capability of being easy-to-use and diminishing pain are the key features to draw the attention of patients suffering from diabetes who are obliged to take insulin daily. Diabetes can be the result of not behaving appropriately to the produced insulin. The other reason stems from the pancreas and its lack of insulin. According to the 2014 survey, about 387 million people have type 2 diabetes that encompasses 90% of all people with this disease. This statistics represents the considerable number of people who have diabetes, which have been contributed to deaths each year ([The Emerging Risk Factors Collaboration, 2010](#)). These are the facts

that bold the significance of researches in the field of drug delivery devices, especially with the goal of pumping insulin. In the early 1980s, Jan Smits was one of the first people who designed micropumps to implant controlled insulin delivery systems in the human body and keeping blood sugar within ideal levels without the need of routine injections.

Among different types of micropumps, those with passive valves have drawn considerable attention. Passive valves reduce the probability of dynamic fatigue and abrasion and are easy to fabricate in micro scales. Nozzle-diffuser valves and Tesla valves are two types of passive valves. In Tesla valves, different flow resistance in forwarding and backward direction causes diodicity. [Stemme \*et al.\* \(1993\)](#) was the first person who developed the idea of using valves with no parts in a nozzle-diffuser piezoelectric micropump. [Forster \*et al.\*](#) exhibited Tesla valves with a better performance compare to nozzle-diffuser model ([Forster \*et al.\* 1995](#)).

[Reed \(1993\)](#) optimized the bypass section of the Tesla model and demonstrated that using two-stage valves approximately doubles the diodicity; and increasing number of stages raises pressure drop, while the diodicity would increase lower. [Forster \*et al.\* \(1999\)](#) demonstrated Tesla valves in microscale and compared them with nozzle-diffuser valves. Furthermore, a new type of micropump has been proposed ([Williams and Forster, 2002](#)), the Tesser valve, having both the features of Tesla-type and nozzle-diffuser. They couldn't prove the priority of the suggested model over other types. According to their research, nozzle-diffuser valves in flows with Reynolds number lower than 100, and Tesla-type valves in flow with Reynolds number higher than were efficient. [Gamboa \*et al.\* \(2005\)](#) utilized numerical solutions and dynamic models to obtain new optimization parameters for Tesla-type valves. Their optimized model had a better diodicity in high Reynolds. [Liao \(2004\)](#) changed the angle of the Tesla valve from 45° to 135° and named it T135. [Kolahdouz \(2010\)](#) made a change in the reunion angle of T135 and achieved a better performance and his model was called MT135. [Mohammadzadeh \*et al.\* \(2013\)](#) showed that the best number of valve stages is two stages and explained the defect of Tesla-type valves in low-Reynolds regimes. [Thompson and Paudel \(2014\)](#) investigated numerically a multistage Tesla valve.

The purpose of producing chemical synthesis has drawn attention to research on the multiphase systems ([Lee \*et al.\* 2005](#); [Shestopalov \*et al.\* 2004](#)). Considerable efforts have been made to improve the performance of the system even for the usage of single-phase flow in a simple configuration. The pros and cons of using multi-phase flow in a micro/nano channel stem from the coexistence of multiple phases, the mitigation in the geometry sizes and the confinement in a channel. The complexity in these multi-phases flows also encompasses controlling the working fluid. The usual pumping method, which is syringe pumping, is difficult to be used in nanochannels because of its higher hydrodynamic resistance. Moreover, the electro-osmotic flow, which is the best option in the single-

phase flow, is not applicable in the multi-phase flow due to the existence of phases. In this regard, some actuation forces such as interfacial are the best option to be utilized in the multiphase flow.

When disparate phases of fluid came together as the adjacent streams, one of them usually wets the walls and lead the other to become as discrete drops ([Utada \*et al.\* 2005](#); [Joanicot and Aidari, 2005](#); [Kawakatsu \*et al.\* 2001](#); [Loscertales \*et al.\* 2002](#)). It shouldn't be forgotten that the stabilization process of flow can be also done by a clear interface ([Hisamoto \*et al.\* 2001](#)) and it is not necessary to account for the gravity in the analysis ([Eijkel and Van Den Berg, 2005](#)).

The aim of devising hydrodynamic stresses in diseases such as diabetes is to obtain the shear stresses in arteries ([Papaharilaou \*et al.\* 2005](#); [Feldman and Stone, 2000](#)). The clotting of red blood cells (RBCs) in arteries lead to atherosclerosis ([Tiwari \*et al.\* 2004](#)). Therefore, numerical and computational methods should be used to better evaluate the vessels for the purpose of designing novel clinical tools. It should be noted that blood is a non-Newtonian fluid and its simulation demands special consideration. Recently ([Weiss \*et al.\* 2006](#)), to demolish the instabilities at low shear stresses, a non-Newtonian fluid (Casson) is used to demolish the instabilities at low shear stresses.:

$$\tau^{0.5} = K_{0c} + K_c (\dot{\gamma})^{0.5} \quad (1)$$

All the investigations over Tesla-type microvalves center on high-Reynolds flow with high pressure-gradients. However, drug delivery systems require few doses of a drug to disperse which call for appropriate diodicity in low pressure-gradients. There has been no research on utilizing Tesla valves in drug delivery micropumps. In this paper, after numerical simulation of the MT135 model and validating the model, the diodicity was studied in a range of different reunion angles (from 128 to 141 degree) to obtain the highest diodicity. Then, by devising the nozzle and diffuser in the bypass way, changing their inlet angles, and some other geometric changes, the diodicity of the valve has been enhanced by approximately 10%. After that, by designing this novel microvalve with the name of TND133 a piezoelectric micropump with two-stage valves was numerically simulated and its function in low frequencies was observed. Contours of velocity depicted and in order to attain a comprehensive study, the usage of non-Newtonian fluid has been analyzed.

## 2. GOVERNING EQUATIONS

In order to assume a fluid as a continuous medium, all of its properties must be continuous. Continuity in a control volume requires at least 104 molecules of the fluid included in the volume and the minimum length for fluids to be continuous is around 8nm. Channel widths in this paper are same as ([Kolahdouz, 2010](#)) equal to 128μm, hence continuity and no-slip condition were satisfied. Mass conservation and momentum equations with

no compressibility in case of Newtonian fluid were:

$$\frac{\partial}{\partial x_j}(\partial U_j) = 0 \quad (2)$$

$$\rho_f \left( \frac{\partial U_i}{\partial t} + U_j \frac{\partial U_i}{\partial x_j} \right) = - \frac{\partial P}{\partial x_i} + \mu_f \left( \frac{\partial^2 U_i}{\partial x_j \partial x_j} \right) \quad (3)$$

Where  $U$  is the velocity of the fluid,  $x$  is the spatial direction,  $P$  represents the pressure of the fluid. The key feature which exhibits the capability of the valve to direct the fluid in the forward direction and its ability to prevent the fluid to flow backward is called diodicity. Due to the fact that valves with no moving are more resistance in the backward direction, even in case of some back pressure, make a forward flow. Diodicity is defined as the ratio between the forward and reverse pressure drop across the valve in constant flow-rate condition (Laser and Santiago, 2004):

$$D_i = \left( \frac{\Delta p_{backward}}{\Delta p_{forward}} \right)_Q \quad (4)$$

### 3. FLOW GEOMETRY AND BOUNDARY CONDITIONS

Both Tesla-type and nozzle-diffuser valves have passive function and the geometry is the factor which makes the pressure drop higher in the backward direction.

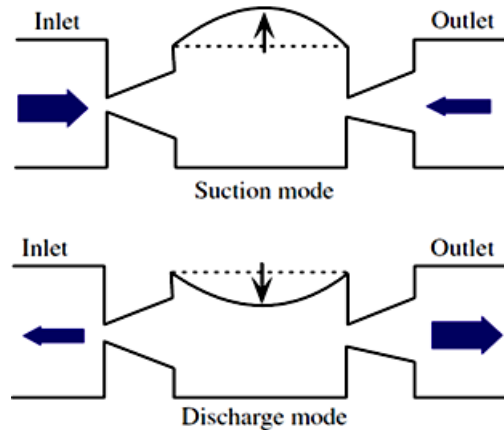


**Fig. 1. A nozzle-diffuser piezoelectric micropump (Nabavi, 2009).**

In the piezoelectric micropumps, two passive microvalves direct the flow and the needed energy to pump the fluid is supplied by a piezoelectric actuator (Nabavi, 2009). The suggested micro-pump consists of two diffusers which are connected to a chamber with an oscillating diaphragm as depicted in Fig. 1, the oscillating diaphragm obliges the fluid to flow through the two diffusers. Consequently, the different resistance toward the forward and reverse direction led the fluid to be pumped. This micro-pump is consisted of two processes, one is the suction mode and the other is the discharge mode. In the former, the membrane moves upward to

enhance the interior volume of the chamber. In this operation the inlet and outlet micro-diffuser acts as a diffuser and nozzle, respectively. In the latter, the diaphragm moves downward to mitigate the interior volume of the chamber. In this process, the micro-diffuser in the inlet and the outlet acts as a nozzle and diffuser, respectively.

These suction and discharge modes lead to a complete pumping cycle for the purpose of transferring fluid from the inlet section to that of outlet. Figure 2 illustrates that in the analogous flow rates of Tesla microvalves, diodicity will be enhanced as the pressure losses in the backward direction in comparison to that of forward, is considerable.

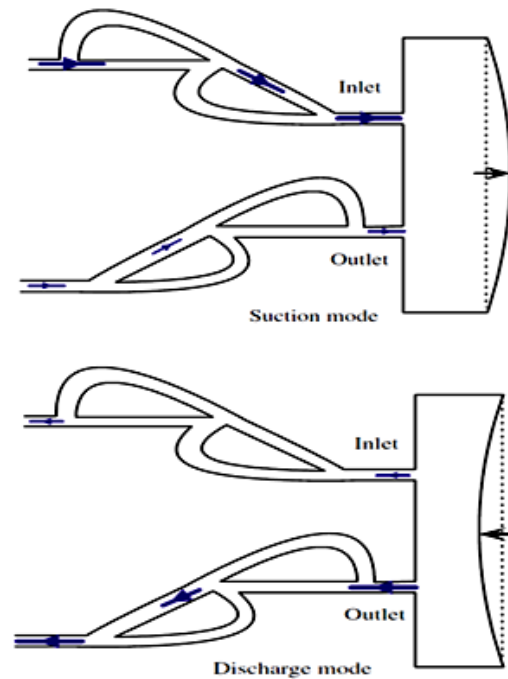


**Fig. 2. A piezoelectric micropump with Tesla-type valves (Nabavi, 2009).**

The difference between these two types of passive valves is that nozzle-diffuser valves are composed of a simple convergent-divergent channel and works due to the difference in cross-section. At small angles of divergence, the pressure drop in the divergent direction is less than the one in convergence. With increasing divergence, fluid separation occurs in a divergent direction and bring about vorticity in the working fluid. This vortex reduces the cross-sectional flow and prevents the flow through the path to the resistance. However, in Tesla valves, the main aspect of diodicity stems from the difference in contact angles of channels. In the forward direction, when the goal is increasing the flow rate, fluid jet crosses the main channel and it is not influenced by the bypass channel. In reverse direction, there exist higher resistance in comparison to forward flow due to the separation and combination of flows in the contact position of the channels. It should be noted that both nozzle-diffuser and Tesla valves are based on the inertial

properties of the flow.

The use of Tesla microvalves has many advantages over other types. For example, one of the major problems of pumping pharmaceutical solutions into the patient's body is the precipitation of the micro/nanoparticles of the fluid at the inlet or outlet sections of the microvalve. This microvalve makes it easy to pump these fluids due to lack of moving parts. Sudden pressure drop in active and some passive microvalves has resulted in large shear stress and blockage of the flow path, which contributes to clotting the blood. It should not be forgotten that phenomena such as fatigue and erosion from moving parts are not altogether with Tesla's microvalve. Furthermore, the process of micro-manufacturing is much easier in these types of microvalves. While existing microvalves do not have the ability to match the high frequencies or they are altogether considerable restrictions, Tesla's type can adapt to high frequencies even to a higher value than the system's resonant frequency.

Nevertheless, it should be noted that the relative proportion of forward flow in comparison to the backward flow has been one of the disadvantages of Tesla microvalves since the invention of its prototype in 1995. If researchers become capable of increasing diodicity and the rate of outflow in these microvalves by using techniques such as changing the geometric parameters, the usage of these passive microvalves will be widespread and older types will be gradually removed from the process of manufacturing.

#### 4. GRID INDEPENDENCY

To numerically simulate MT135, vertex coordinates of the valve were extracted by the Digitizer software due to its complicated geometry. By transporting information to CAD software, 2D shape modeling was done. Meshing the geometry was performed with quad elements. By importing the mesh file into Mesh generator and establishing boundary elements similar to (Kolahdouz, 2010), MT135 was remodeled. To obtain the correctness of the geometry and mesh, grid independency analysis has been performed. As indicated in Fig. 3, the velocity of outflow will be increased by making more cells and, consequently, more nodes. This route continues until the geometry achieves the approximate number of 89182 nodes. If this value continues to become higher, the proposed mesh would be improper. However, by adding more nodes to the suggested structure, the velocity in outflow reach to a constant value that corroborates the correctness of the proposed mesh structure.

#### 5. NUMERICAL ANALYSIS

In order to become assured of the proposed model and its validity, the simulated results of the MT135 become compared with the experimental reports of the Kolahdouz (2010). Figure 4 represents the changes in the diodicity of the valve by the changes in the pressure gradient.

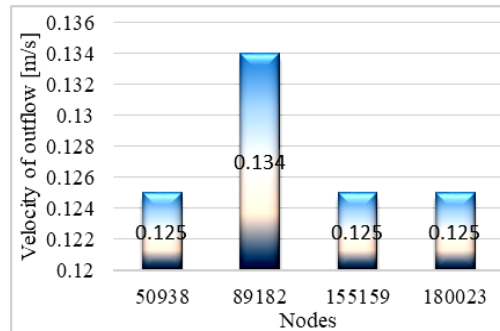


Fig. 3. Grid independency of the mesh structure.

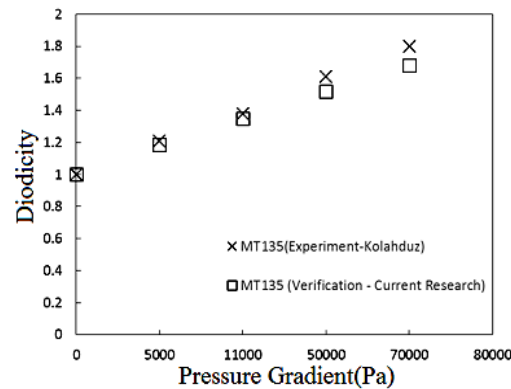


Fig. 4. Scaling of the diodicity with the pressure gradient in the MT135 model.

As it can be seen, by increasing the pressure gradient of the microvalve, the difference between experimental and simulation results become higher and in the pressure gradient of 70 kPa, Error becomes to 6.6%. The first reason of this difference stems from the existing errors in residual values of the simulation. Secondly, the geometry of the inlet fluid reservoir to the micropump has not been specified in numerical analysis and, consequently, the fluid flow in the inlet is not fully developed. Thirdly, the resulting errors from calculating the pressure gradient by mass flow rate can be an effective factor. At last but not least, existing tolerances of the prototype, which are the result of micro-machining, are the other reason for this difference.

The point to make was that the diodicity in the MT135 which was the last optimized version of Tesla-type valves was very small in low-pressure gradients. In Fig. 5, the design parameters of a Tesla microvalve is shown. Therefore, a range of  $\alpha$  angles which was set as the complement of the  $\beta$  in (Kolahdouz, 2010), where studied to investigate the effects of  $\alpha$  on diodicity.

The range was from  $128^\circ$  to  $141^\circ$  with  $1^\circ$  steps. Insulin was set as the fluid and diodicity was numerically extracted by flow solver. To calculate the diodicity for each case, the outlet pressure was set higher than the inlet pressure; after calculating the solution, the computed flow rate was set as the initial condition for the inlet and by setting the outlet pressure to zero, forward flow was calculated. By considering the pressure gradient of the last part, and the desired initial pressure gradient, diodicity of

each case in similar flow rates were computed. Diabetes patients take a different dose of drugs depending on the type of diabetes they suffer from. Among patient who is obliged to needle injection, different doses of insulin are prescribed, most of whom have to take from 10 to 15 units of different types of insulin daily and the maximum dosage may reach to 60 units per day. One cubic centimeter volume of insulin equals 100 units. So the desired flow rate for the insulin delivery micropump should be in the order of 1 unit of insulin. Different neutral solutions of zinc insulin and their properties are presented in Table 1.

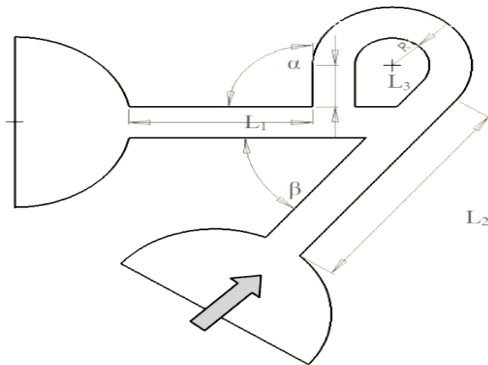


Fig. 5. Design parameters in a Tesla valve.

Table 1 mechanical properties of neutral regular insulins at 20 ac (Brange, 2012)

	Insulin concentration IU/ml		
	0	40	80
Viscosity (cp)	1.01	1.02	1.02
Density (g/ml)	1.005	1.006	1.006

## 6. RESULTS AND DISCUSSION

Numerical analysis of diodicity in different  $\alpha$  conditions showed that the highest diodicity is by far belongs to  $\alpha = 133^\circ$ . Furthermore,  $\alpha = 141^\circ$  and  $\alpha = 132^\circ$  the diodicity is approximately more than other points as shown in Fig. 6.

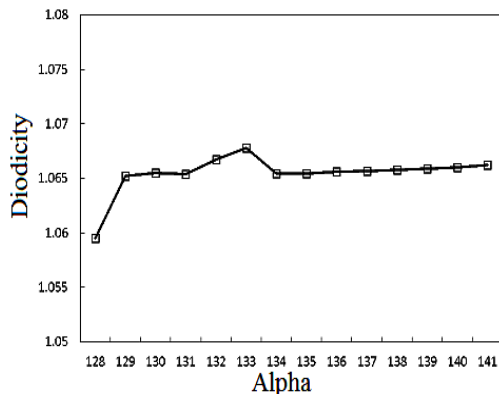


Fig. 6. Scaling of the diodicity with different  $\alpha$  values.

However, there is less than 0.5% difference in the diodicity of  $133^\circ$  and  $135^\circ$  case. In the next step, inspired by nozzle-diffuser tesla valves, two angles were set in the bypass section of the valve, forming a diffuser and a nozzle. In Fig. 7 these two angles are delineated

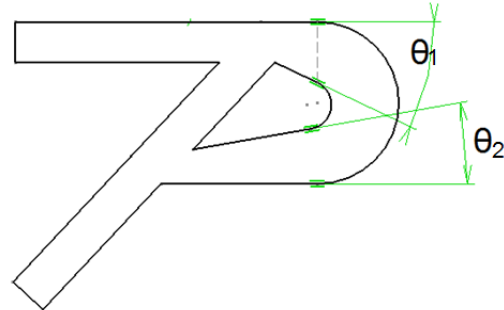


Fig. 7. The nozzle and the diffuser design of the bypass section of the Tesla valve.

Different values of  $\theta_1$  were modeled on the basis of an increase in the width of the valve. By increasing width of the bypath section by 10%, 20%, 40%, 50%, 60%, 80%, 100% of the initial width, diodicity in each case was numerically analyzed. In Fig. 8, by increasing  $\theta_1$ , the fluid entering the bypass section encountered a diffuser and as a result, a pressure drop occurred due to the increased width of the flow path. The point is, like nozzle-diffuser valves, the pressure drop through a diffuser is less than pressure drop through a nozzle. So the  $\theta_1$  created in the path decreased the flow through the bypass section in reverse direction. This fact gained us the most diodicity among studied cases in  $\alpha=25.5^\circ$  which resulted in 50% increase in the width of the bypass section.

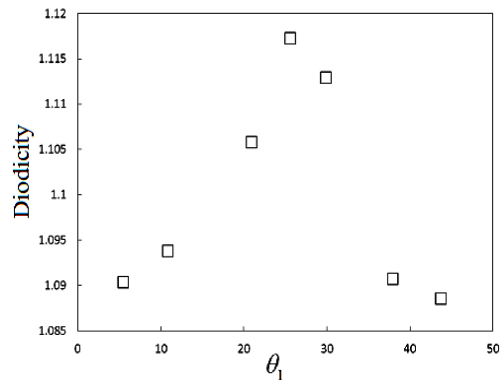
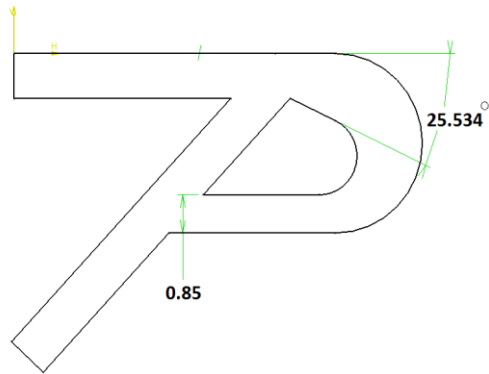


Fig. 8. Scaling of the diodicity with different  $\theta_1$  values.

In the next step, in order to bring about more pressure drop in the reverse flow, the width of the Y-shaped section in the bypass area was decreased to 85% of the main case as shown in Fig. 9. Due to DRIE (Deep Reactive Ion Etching) restrictions, it was preferred not to decrease the width less than  $100\mu\text{m}$ . This change caused a very little increase in the diodicity of the valve. After that, by increasing the value of  $\theta_2$ , diodicity of the valve was investigated.



**Fig. 9. Decreased width of the Y-shaped section of the valve in bypass area.**

The limitation was that decreasing the  $\theta_2$  more than  $12^\circ$  would diminish the inner radius of the bypass section too much. Therefore a few cases  $\theta_2$  should be examined. Figure 10 shows the diodicity with different values of  $\theta_2$ .

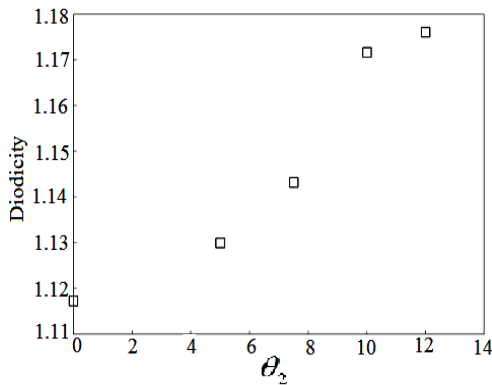
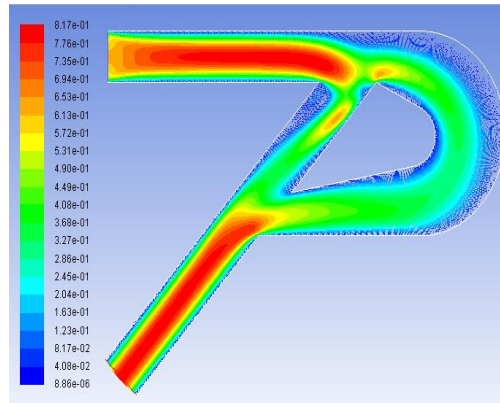


**Fig. 10. Scaling of the diodicity with different values of  $\theta_2$ .**

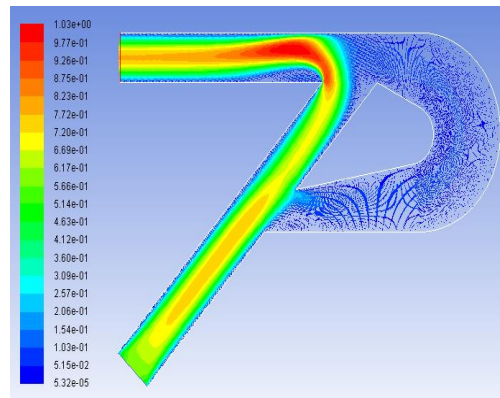
The examined angles  $\theta_2$  were  $5^\circ$ ,  $7.5^\circ$ ,  $10^\circ$  and  $12^\circ$  and as shown in Fig. 10,  $\theta_2 = 12^\circ$  resulted in the most diodicity, however, because of DRIE restrictions and due to little difference between the diodicity of this case and the  $\theta_2 = 10^\circ$  case, the latter condition was chosen. This change in the Y-shaped section makes the reverse flow to enter the bypass section due to the increased flow section which results in more flow contrast in the reunion T-shaped section of the valve and boosts the pressure drop in that area.

The final result for the diodicity was a 9.97% increase compared to the MT135. The resulted diodicity was 1.176107 in a 10.06 mg/s flow rate condition. Figures 11 and 12 show velocity contours of the proposed microvalve in forward and reverse flow respectively. It is shown that in the reverse flow, the fluid hits the wall of the valve in the T-shaped area which causes a significant pressure drop. In Fig. 13, scaling of the mass flow rate of the designed valve with different pressure inlet values is depicted. It is obvious that in low-pressure values, there is approximately a linear relation between two

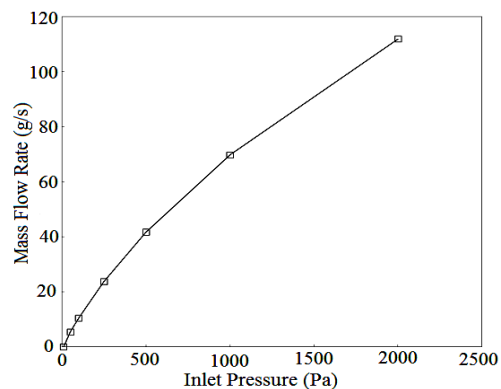
parameters. This can be considered as a key factor to control the mass flow rate of the valve, just by controlling the inlet pressure. When the pressure increases, the velocity of the flow gets higher values and as a result, dynamic frictions which have a relation with velocity raised by the power of two, will increase and so the rate of the flow will decrease.



**Fig. 11. Velocity [m/s] contour in forwarding flow in a case of 100Pa pressure gradient.**



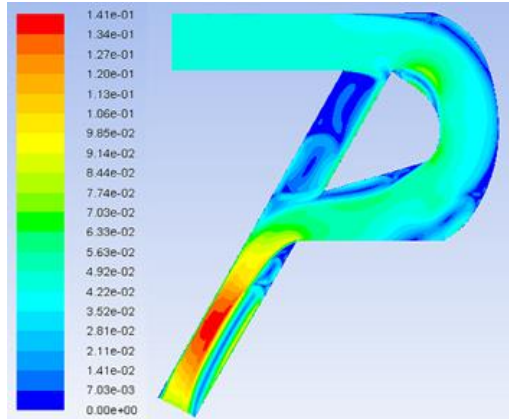
**Fig. 12. Velocity [m/s] contour in reverse flow in a case of 100Pa pressure gradient.**



**Fig. 12. Scaling of the mass flow rate of the designed valve with inlet pressure values.**

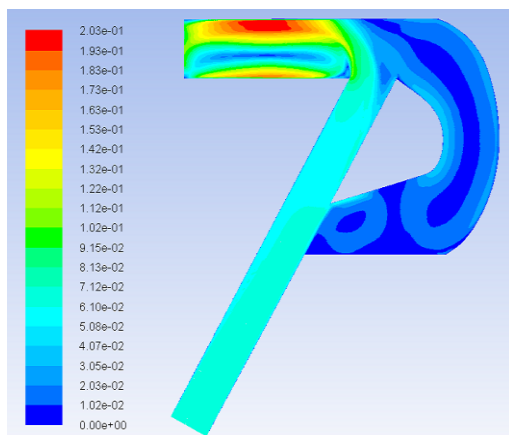
Recently, for the purpose of devising better cooling capability of the micro-technologies, two-

phase heat transfer has been utilized in this field. The previous heat transfer studies in this field is somewhat restricted to vaporization in macro channels, and they are not appropriate for the small-scale microchannel studies. Moreover, multiphase fluid flow behavior is totally different from that of single-phase. Figure 14 shows the velocity contours in the forward flow of water and air.



**Fig. 13. Velocity [m/s] contours in the forward flow of water and air.**

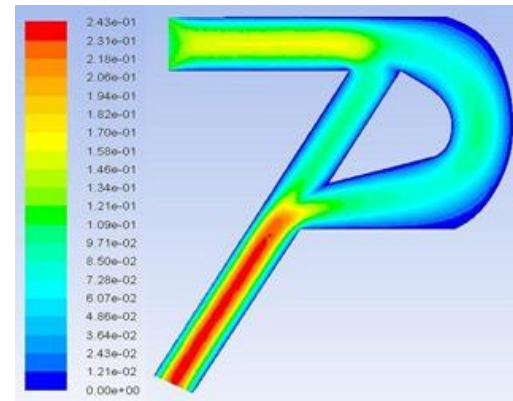
The illustration simply delineates that the behavior of the single-phase flow of water is different from multi-phase one. Noted that in this analysis the dominant fluid is water and air is the second fluid. According to (Shui *et al.* 2007), this kind of flow classified as stratified flow. To show the difference in velocity behavior of multi and single-phase flows in backward flow, Fig. 15 is presented.



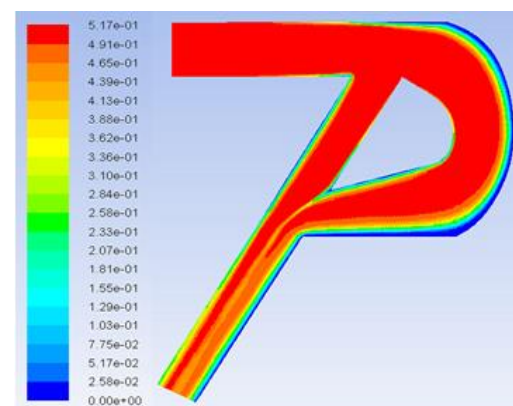
**Fig. 14. Velocity [m/s] contours in backward flow of water and air.**

Figure 15 simply illustrates a vortex kind phenomenon of flow at the exit of the micropump which is totally different from usual single-phase flow of water in this micropump. The importance of studying non-Newtonian is to understand blood behavior. For instance, the velocity study of blood lead to better understanding of circulatory phenomena. It means, by having a

threshold of pressure can lead to a partial "blockage" in some vessels, because of the pathological change in the yield stress. For further enlightenment, an investigation of multi-phase flow by an arbitrary Non-Newtonian Casson fluid is presented; Figure 16 shows the velocity contours of this flow Figure 16 simply shows that any kind of circulation doesn't occur and this kind of micropump is appropriate for transferring blood and other kinds of fluids. This confirms that the non-Newtonian effect of Casson, has reduced the distortion of flow pattern and, therefore, as the wall shear stress, in this case, is higher than that of air and water, the gas blockage would not happen at the outlet of the microvalve. This phenomenon verifies that local pressure drop by the usage of non-Newtonian fluid across the microvalve is higher in magnitude than that of Newtonian. In general, the non-Newtonian viscosity has resulted in a flatter velocity contour than the Newtonian viscosity. Figure 17 shows the phase contours of water in the forward flow of water and Casson.



**Fig. 15. Velocity [m/s] contours in the forward flow of water and Casson.**



**Fig. 16. Volume fraction of water in the forward flow of water and Casson.**

According to (Shui *et al.* 2007), this kind of flow classified as stratified flow too. To study the backward flow of this Non-Newtonian multi-phase flow, the velocity contours of this kind of flow is illustrated in Fig. 18.

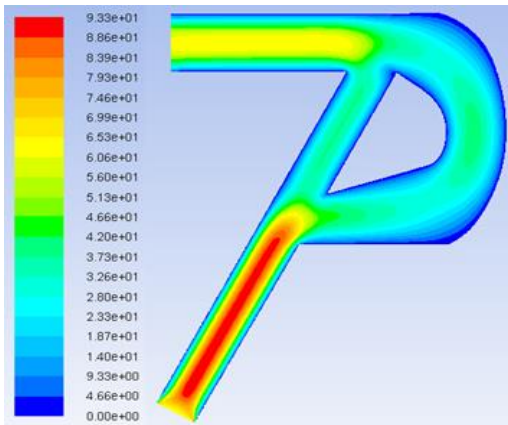


**Fig. 17. Velocity [m/s] contours in backward flow of water and Casson.**

There isn't a noticeable change in the profile of backward and forward flow in the multi-phase investigation of water and Casson; so it can be concluded that there isn't enough diodicity in a Non-Newtonian multi-phase flow of this kind of micropumps. Figure 19 delineates the phase contours of water in backward flow of water and Casson. As it can be seen, by using a non-Newtonian fluid such as Casson, which benefits from higher viscosity, the movement of water through backward direction has reduced. Previously in Fig. 17 it has been shown that moving the multi-phase flow toward the forward direction has no restriction.

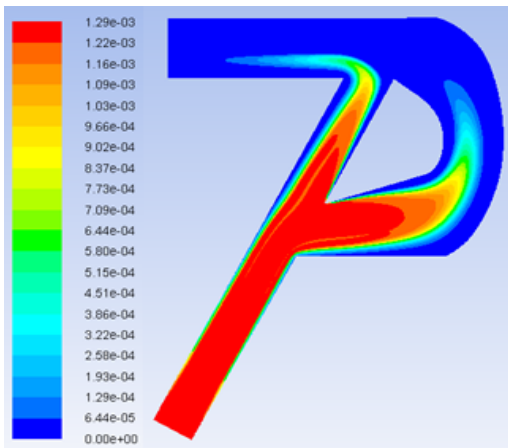


**Fig. 18. Volume fraction of water in backward flow of water and Casson.**

The designed microvalve was modeled in a two-stage condition as the inlet and outlet of a piezoelectric microvalve to direct the flow from the inlet through the micropump chamber to the outlet. The 3D model meshing was performed in a structured way using hex elements which resulted in 1131300 elements (Fig. 20).

The numerical simulation was performed in transient mode, therefore, Coupled Pressure-Velocity was used. Least squares cell-based method was utilized for spatial discretization of the gradient, and pressure and momentum equations were discretized by the second-order scheme. Depending

on the frequency of each case, the time step was set as 0.0625 of a period. For instance, in the case of 100Hz, time step was set to 0.000625 seconds. Figure 21 shows the successful pumping of the fluid by the piezoelectric micropump with designed microvalves in the frequency of 50Hz.

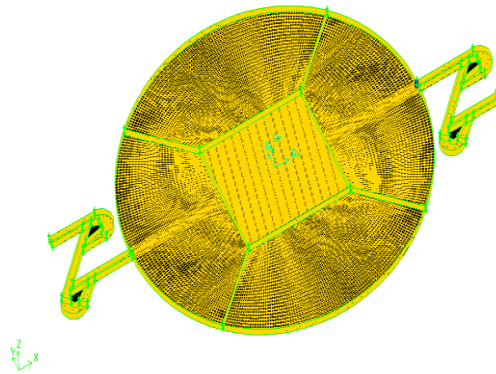


**Fig. 19. 3D model of the micropump.**

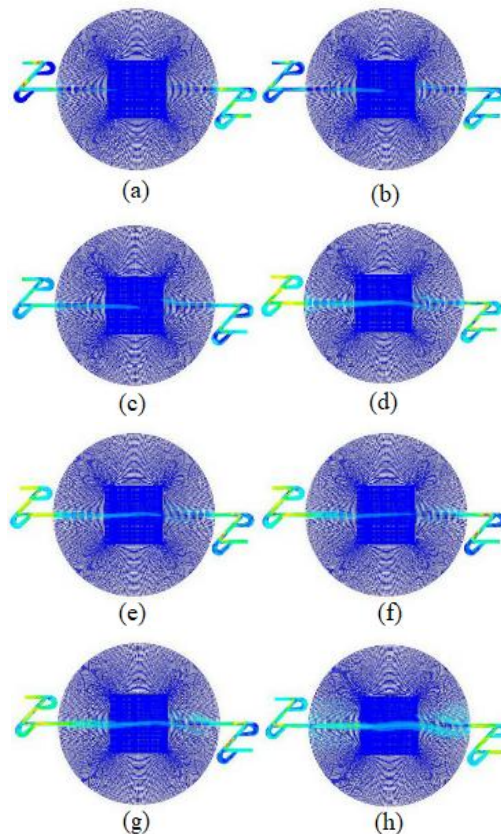


**Fig. 20. Velocity contours in the micropump with designed microvalves in 50Hz frequency. (a) 0.00125 [s], (b) 0.0025 [s], (c) 0.00375 [s], (d) 0.005 [s], (e) 0.00625 [s], (f) 0.75 [s], (g) 0.875 [s], (h) 1 [s].**

In Fig. 22 scaling of the diaphragm movement frequency with the maximum mass flow rate is shown. In low frequencies, there is a linear relation between this two parameters. As it can be seen,

in Fig. 22 (a), the micropump has started to pump the working fluid into the diaphragm and, consequently suction is going to happen. It should be noted that the mass flow rate in this step is higher in the right microvalve due to previous discharging. As time goes by, the mass flow rate from the diaphragm increases and in the Fig. 22 (h) it reaches its maximum. Moreover, the mass flow rate in the left microvalve constantly rises as all these figures are in suction mode. In the right microvalve, however, the mass flow rate decreases at first until 0.00375 (s) in Fig. 22 (c), which is related to the previous discharging. After that the value of the mass flow rate increases in this microvalve. A noticeable observation in these figures is that although studying is in suction mode, there exists considerable backward mass flow rate. This verifies the previously stated remark that the relative proportion of forward flow in comparison to the backward flow is one of the Tesla microvalves' disadvantages in the application of piezoelectric micropumps. One of the most important features of the drug delivery systems is the capability of being controlled to disperse a precise dose of drug into the patient's body. This figure demonstrates that controlling frequency is a mean of controlling the mass flow rate in the micropump.

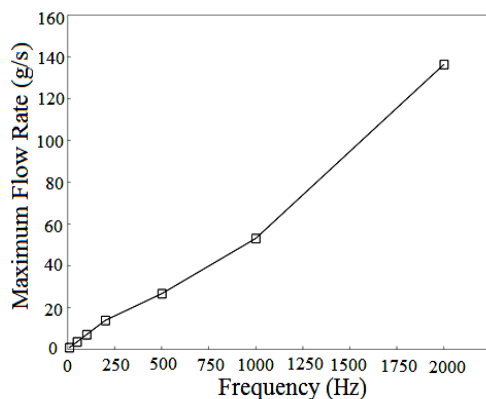


**Fig. 21. Scaling of the diaphragm movement frequency with a maximum mass flow rate.**

## 7. CONCLUSION

In this article, diodicity of a Tesla microvalve in low-pressure gradients was boosted by numerical solutions over making changes in the geometry of the valve based on nozzle-diffuser valve models. Different  $\alpha$  angles of the Tesla-type valve, MT135, were studied and in  $133^\circ$  the highest value was reached. Then by creating a nozzle and a diffuser in the bypass section of the Tesla valve, 9.97 and increase in the diodicity was gained. A 3D model of the micropump with designed microvalves was numerically simulated and results showed the successful performance of the micropump to be used as an insulin delivery device, working in low flow rate regimes. Furthermore, a multiphase flow of water and air achieved and results showed circulating flow near the outlet in a backward mode which totally inappropriate for transferring blood as a Non-Newtonian fluid; thus, the multiphase flow of

water and Casson attained and although results don't show any diodicity in micropump it's proper for transferring blood.

## REFERENCES

- Brange, J. (2012). Galenics of insulin: the physicochemical and pharmaceutical aspects of insulin and insulin preparations. Springer.
- Eijkel, J. C. T. and A. Van Den Berg (2005). Nanofluidics: what is it and what can we expect from it?. *Microfluidics and Nanofluidics* 1(3), 249-267.
- Feldman, C. L. and P. Stone (2000). Intravascular hemodynamic factors responsible for the progression of coronary atherosclerosis and development of vulnerable plaque. *Current Opinion in Cardiology* 15(6), 430-440.
- Forster, F. K., R. L. Bardell, A. P. Blanchard, M. A. Fromowitz and N. R. Sharma (1999). *Micropumps with fixed valves*. US Patents.
- Forster, F. K., R. L. Bardell, M. A. Fromowitz, N. R. Sharma and A. P. Blanchard (1995). Design, fabrication and testing of fixed-valve micropumps. *Proceedings of the ASME Fluids Engineering Division*, 234.
- Gamboa, A. R., C. J. Morris and F. K. Forster (2005). Improvements in Fixed-Valve Micropump Performance through Shape Optimization of Valves. *Journal of Fluids Engineering* 127(2), 339.
- Hisamoto, H., T. Saito, M. Tokeshi, A. Hibara and T. Kitamouri (2001). Fast and high conversion phase-transfer synthesis exploiting the liquid-liquid interface formed in a microchannel chip. *Chemical Communication* (24), 2662-2663.
- Joanicot, M. and A. Ajdari (2005). Droplet control for microfluidics. *Science* 309(5736), 887-888.
- Kawakatsu, T., G. Trägårdh, Ch. Trägårdh, M. Nakajima, N. Oda and T. Yonemoto (2001). The effect of the hydrophobicity of microchannels and components in water and oil phases on droplet formation in microchannel water-in-oil emulsification. *Colloids and Surfaces A* 179(1), 29-37.
- Kolahdouz, E. M. (2010). *Design and fabrication of a piezoelectrically actuated micropump using modified Tesla type microvalves*. MSc Thesis, Isfahan University of Technology, Isfahan, Iran.
- Laser, D. J. and J. G. Santiago (2004). A review of micropumps. *Journal of Micromechanics Microengineering* 14(6), 35-64.
- Lee, C. C., G. Sui, A. Elizarov, C. J. Shu, Y. S. Shin and A. N. Dooley (2005). Multistep synthesis of a radiolabeled imaging probe using integrated microfluidics. *Science* 310(5755), 1793-1796.
- Liao, P. F. (2004). *A study on no-moving-part*

- valves for flows in microchannels*. MSc thesis, Department of Aeronautics and Astronautics. National Cheng Kung University, Taiwan.
- Loscertales, I. G., A. Barrero, I. Guerrero, R. Cortijo, M. Marquez and A. M. Gañán-Calvo (2002). Micro/nano encapsulation via electrified coaxial liquid jets. *Science* 295(5560), 1695-1698.
- Mohammadzadeh, K., E. M. Kolahdouz and E. Shirani (2013). Numerical study on the performance of Tesla-type microvalve in a valveless micropump in the range of low frequencies. *Journal of Micro-Bio Robotics* 8(3), 145-159.
- Nabavi, M. (2009). Steady and unsteady flow analysis in micro-diffusers and micropumps: A critical review. *Microfluidics and Nanofluidics* 7(5), 599-619.
- Papaharilaou, Y., J. A. Ekaterinaris, E. Manousaki and N. Katsamouris (2005). Stress analysis in abdominal aortic aneurysms applying flow induced wall pressure. Fifth GRACM International Congress on Computational Mechanics, Limassol, Cyprus, 29 June- 1 July.
- Reed, J. L. (1993). *Fluidic rectifier*. US Patents.
- Shestopalov, I., J. D. Tice and R. F. Ismagilov (2004). Multi-step synthesis of nanoparticles performed on millisecond time scale in a microfluidic droplet-based system. *Lab on a Chip* (4), 316-321.
- Shui, L., J. C. T. Eijkel and A. Van den Berg (2007). Multiphase flow in micro-and nanochannels. *Sensors and Actuators B: Chemical* 121(1), 263-276.
- Stemme, E. and G. Stemme (1993). Valve-less fluid pump. *Swedish Patent Application* 9, 300.
- The Emerging Risk Factors Collaboration* (2010). Diabetes mellitus, fasting blood glucose concentration, and risk of vascular disease: a collaborative meta-analysis of 102 prospective studies. *The Lancet* 375(9733), 2215-2222.
- Thompson, S. M. and B. J. Paudel (2014). Numerical investigation of multistaged tesla valves. *Journal of Fluids Engineering* 136(8).
- Tiwari, P., P. S. Antal, A. Burgoyne, G. Belfort and M. Z. Podowski (2004). Multifield computational fluid dynamics model of particulate flow in curved circular tubes. *Theoretical and Computational Fluid Dynamics* 18(2), 205-220.
- Utada, A. S., E. Lorenceau, D. R. Link, P. D. Kaplan, H. A. Stone and D. A. Weitz (2005). Monodisperse double emulsions generated from a microcapillary device. *Science* 308(5721), 537-541.
- Weiss, M., B. Plosz, K. Essemiani and J. Meinhold (2006). *Sedimentation of activated sludge in secondary clarifiers*. 5<sup>th</sup> World Congress of Particle Technology (WCPT), Orlando, Florida, USA, 23-27.
- Williams, B. E. and F. K. Forster (2002). Parametric Design of Fixed-Geometry Microvalves: The Tesser Valve. *ASME*, 431-437.